Colloid & Polymer Science Colloid Polym Sci 272:478–486 (1994)

Adsorption and desorption of colloidal particles on glass in a parallel plate flow chamber – Influence of ionic strength and shear rate

J. M. Meinders and H. J. Busscher

Laboratory for Materia Technica, University of Groningen, The Netherlands

Abstract: The adsorption and desorption rates of 736 nm diameter polystyrene particles on glass were studied *in situ* using a parallel plate flow chamber and automated image analysis. Adsorption and desorption rates were measured simultaneously during deposition, enabling the determination of initial deposition rates, blocked areas per particle, desorption rate coefficients, and the number of adhering particles in the stationary state. Deposition experiments were done from suspensions with different potassium nitrate concentrations (1, 10 and 50 mM) and at varying shear rates (15 to 200 s^{-1}). The initial deposition rate, the desorption rate, the blocked area per particle and the number of adhering particles in the stationary state showed major variations with the shear rate and the ionic strength of the suspension. At low ionic strength, the number of adhering particles showed an oscillatory behavior in time, presumably due to a varying interaction between particle and collector surface. Blocked areas, determined from deposition kinetics, ranged 705 to 2374 cross-sections at low ionic strength, and from 10 to 564 at high ionic strength, and corresponded well with those estimated from local pair distribution functions which were obtained from an analysis of the spatial arrangement of the adhering particles.

Key words: Parallel plate flow chamber – adsorption – desorption – blocked area – image analysis

Introduction

Adsorption and desorption of colloidal particles adhering on collector surfaces are of importance in many fields of application such as filtration, separation, flocculation, marine fouling, and adhesion of microorganisms to surfaces. Deposition is a non-linear process in time, among other factors due to "blocking" and desorption. When a particle adheres to a surface, it blocks an area around it and this leads to a reduction in the deposition rate with time. Alternatively, desorption of particles during deposition will also lead to a net reduction in the overall rate of deposition [1–8].

The area blocked by an adhering particle, usually expressed in terms of particle cross-sectional areas, depends not only on the particle size, but also on the electrostatic forces and hydrodynamic conditions near an adhering particle [9–11]. In a relatively simple analysis, the blocked areas are assumed not to overlap, hence, the excluded area varies linearly with the number of adhering particles. However, Schaaf and Talbot [4] considered that during coverage, blocked areas can overlap, thus reducing the average blocked area per particle, and this results in an additional non-linearity in the deposition process [12].

As stated above, desorption also contributes to non-linearity during deposition. Moreover, in order to be able to experimentally measure the blocked areas from the deposition kinetics, the actual desorption rates have to be known. Experimental setups designed to measure adsorption and desorption rates are mostly based on first performing an adsorption experiment after which

flow without particles is started to enter the desorption phase of the experiment [13–15]. However, this procedure tends to underestimate the desorption rate since in an actual process of adhesion and desorption, there are collisions between flowing and adhering particles and this would increase the desorption rate [3]. Therefore, simultaneous measurement of adsorption and desorption rates is essential for an accurate calculation of the blocked area from deposition kinetics.

Sjollema et al. [16] described a system, based on a parallel plate flow chamber and image analysis, in which a real time enumeration of adhering particles *in situ* can be performed. *In situ* enumeration avoids passing of the sample with adhering particles through liquid-air interfaces, a procedure that exerts relatively high shear forces on the adhering particles and that may stimulate detachment of an unknown number of particles. Modification of the program, i.e., comparison of successively grabbed images yielding the time of arrival and departure of each individual adhering particle, has allowed us to determine adsorption and desorption rates simultaneously, resulting in a more accurate measurement of the deposition kinetics [8].

In our previous work [8], we have investigated the adsorption and desorption of polystyrene latex particles on glass at various flow rates (0.034 to 0.456 ml s^{-1}) and at two ionic strengths (1 and 60 mM KNO_3). In these experiments the number of particles in the suspension was kept constant (3.0×10^8 ml^{-1}). In this paper we have extended our work to study the effect of particle number concentration. We have also carried out experiments at three ionic strengths (1, 10 and 50 mM KNO_3). The results obtained in this work were compared and contrasted with the previous report [8].

Materials and methods

Polystyrene particles, collector material and experimental conditions

Monodisperse polystyrene particles (UV-148, AKZO Research, Arnhem, The Netherlands) with a diameter of 736 nm were kindly provided by Dr. R. Zsom, AKZO, The Netherlands. Particles were washed two times by centrifugation in demineralized water and suspended to a concentration of around 2×10^8 ml in a 1 mM, 10 mM or 50 mM potassium nitrate [KNO_3] solution at pH 7.0. The surface characteristics as well as the preparation of the polystyrene latices have been described by Brouwer and Zsom [17].

Glass plates, used as collector material, were extensively washed with a surfactant RBS in demineralized water, followed by alternately rinsing with methanol and demineralized water. After this cleaning procedure, a zero water contact angle was observed on all plates. The surface characteristics of thus prepared glass plates have been described in detail by Sjollema and Busscher [18].

Experiments with different ionic strengths were done in duplicate at different flow rates ranging from 0.034 ml s^{-1} to 0.456 ml s^{-1}, corresponding with shear rates ranging from 15 s^{-1} to 200 s^{-1} and Reynolds numbers ranging from 0.9 to 12.0, well within the range of laminar flow.

Parallel plate flow system and image analysis

The deposition experiments were carried out in a parallel plate flow chamber, which has been described by Sjollema et al. [16]. As an important feature, the flow chamber, with dimensions $16 \times 8 \times 1.8$ cm, has a gradually changing inlet and outlet region. This facilitates the establishment of laminar flow in the centre of the chamber. The bottom and top plates, with dimensions of 5.5×3.8 cm, are made out of glass. A Teflon spacer in between the two plates, yields a separation distance of 0.06 cm. A pulse free flow was created by hydrostatic pressure and the suspension was recirculated by a roller pump.

The entire flow chamber is placed on the stage of a phase contrast microscope (Olympus BH-2) equipped with a 40 × objective with an ultra long working distance (Olympus ULWD-CD Plan 40 PL). A CCD camera (CCD-MX High technology, Eindhoven, The Netherlands) is mounted on the phase contrast microscope and is coupled to an image analyzer (TEA, image-manager, Difa, Breda, The Netherlands), installed in a 33 MHz IBM AT personal computer. With this set-up, a direct observation of the deposition process *in situ* is possible without any additional shear forces acting on the deposited particles. Full details of the experimental set-up were given in [8].

Enumeration of the total number of adhering particles as well as of the number of adsorbing and desorbing particles was carried out on the bottom plate of the flow chamber according to the method described by Meinders et al. [8, 19]. Briefly, during deposition images are grabbed and, after background subtraction, Laplace filtering and thresholding, stored on disk. Further analysis consisted of comparison of successively stored images, resulting in the total number of adhering particles and the total number of adsorbed and desorbed particles as a function of time.

Data analysis

The deposition rate $j(t)$ of colloidal particles to collector surfaces can be expressed as

$$j(t) = j_{ads}(t) - j_{des}(t) , \tag{1}$$

in which $j_{ads}(t)$ and $j_{des}(t)$ are the adsorption and desorption rates, respectively.

Neglecting residence time effects, i.e., assuming that the desorption probability of an adhering particle does not depend on the time during which a particle has been adhering to the collector surface, the desorption rate $j_{des}(t)$ can be described as

$$j_{des}(t) = \beta n(t) , \tag{2}$$

in which β is the desorption rate coefficient and $n(t)$ the number of adhering particles on a collector surface at time t [1, 8].

The adsorption rate decreases due to blocking effects and can be expressed as

$$j_{ads}(t) = j_0(1 - A_1 n(t)) , \tag{3}$$

in which j_0 is the initial deposition rate and A_1 the area blocked by an adhering particle. In Eq. (3), A_1 is considered to be independent of the number of adhering particles and is usually expressed as a factor γ, according to

$$A_1 = \pi a^2 \gamma , \tag{4}$$

with a being the particle radius. [1,8].

Equations (1–3) can be combined [8] to yield expressions for the number of adhering particles, the total number of adsorbed particles and the total number of desorbed particles (Eqs. (5–7), respectively).

$$\begin{aligned} n(t) &= \int_0^t j(t')\,dt' \\ &= \frac{j_0}{A_1 j_0 + \beta}(1 - e^{-(A_1 j_0 + \beta)t}) \\ &= n_\infty(1 - e^{-(A_1 j_0 + \beta)t}) \end{aligned} \tag{5}$$

$$\begin{aligned} n_{ads}(t) &= \int_0^t j_{ads}(t')\,dt' \\ &= \frac{j_0}{A_1 j_0 + \beta}\left[\beta t + \frac{A_1 j_0}{A_1 j_0 + \beta} \times (1 - e^{-(A_1 j_0 + \beta)t})\right] \end{aligned} \tag{6}$$

$$\begin{aligned} n_{des}(t) &= \int_0^t j_{des}(t')\,dt' \\ &= \frac{\beta j_0}{A_1 j_0 + \beta}\left[t - \frac{1}{A_1 j_0 + \beta} \times (1 - e^{-(A_1 j_0 + \beta)t})\right] \end{aligned} \tag{7}$$

j_0, A_1, β, and a delay time t_0 (the time required for focusing the microscope for image analysis after the start of the experiment) were determined by an iterative least square fitting procedure of Eqs. (5–7) to $n(t)$, $n_{ads}(t)$ and $n_{des}(t)$, respectively. First estimates of j_0 and n_∞ are used as input parameters for a least square fit of Eq. (5) to $n(t)$, yielding new estimates of j_0, $(A_1 j_0 + \beta)$ and t_0. Using t_0 as input parameter for the least square fit of Eq. (6) to $n_{ads}(t)$, while keeping j_0 and $(A_1 j_0 + \beta)$ fixed, yields new estimates of A_1, β and t_0. Using β as input parameter for the least square fit of Eq. (7) to $n_{des}(t)$, while keeping j_0 and $(A_1 j_0 + \beta)$ fixed, yields a new estimate of β. Subsequently, this fitting procedure is repeated, while using the new estimates of j_0 and A_1 and the average values of t_0 and β, obtained from the fits of Eqs. (5–7). The entire procedure is repeated until the parameters fitted remain unchanged within 10^{-4}%.

Results

Figure 1 shows the results for the total number of adhering particles n, the adsorption rate

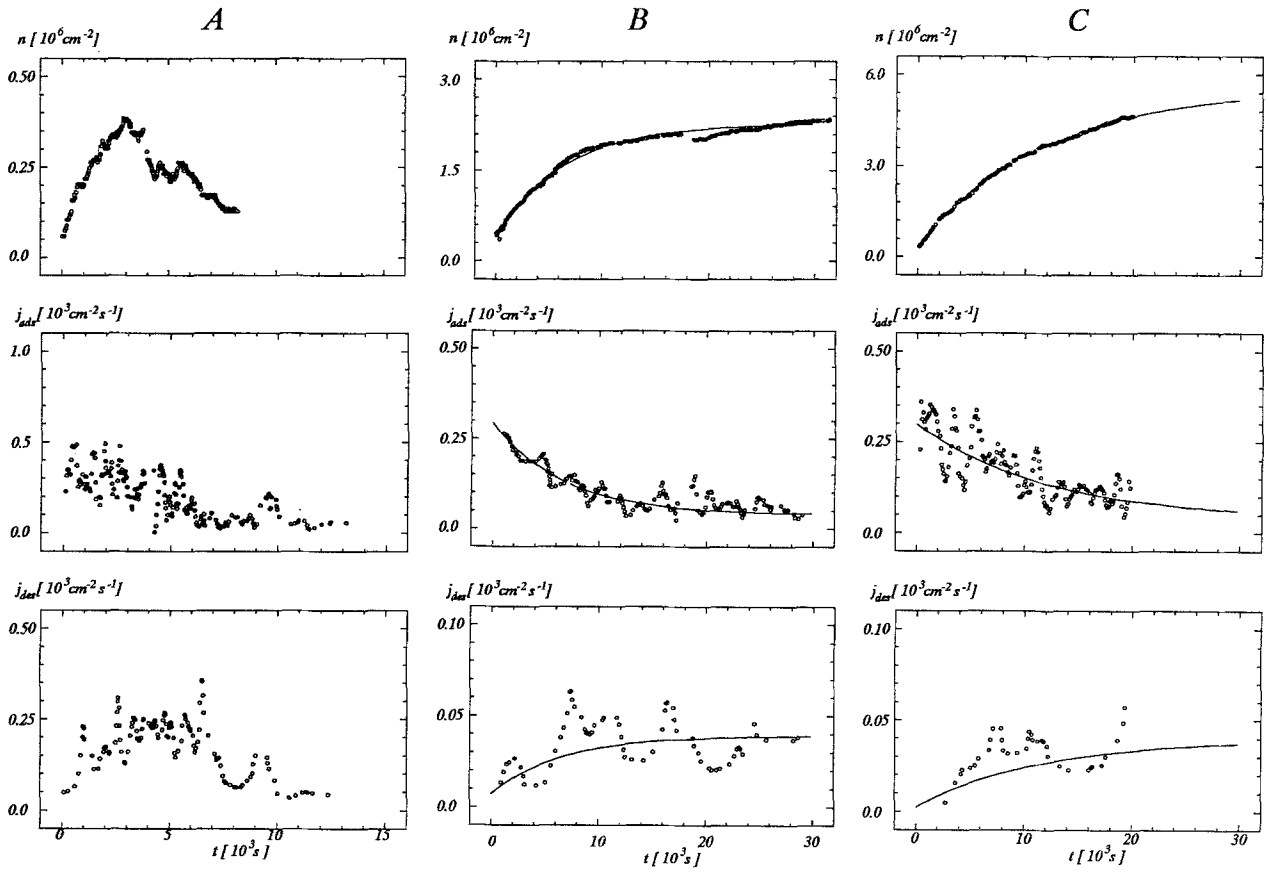

Fig. 1. Illustration of the total number of adhering particles $n(t)$, the adsorption rate $j_{ads}(t)$, and the desorption rate $j_{des}(t)$ for deposition of polystyrene particles on a glass collector during deposition as a function of time for an ionic strength of 1 mM (1a), 10 mM (1b), and 50 mM (1c) for a shear rate of 50 s^{-1}. The drawn lines represent the best fit of Eqs. (5–7) to the data points

j_{ads} and the desorption rate j_{des} as a function of time, for the three ionic strengths employed (1, 10, and 50 mM KNO_3) and at a shear rate of 50 s^{-1}. Our results at 1 mM KNO_3 show an increase in number of adhered particles with time, reach a maximum at $t \approx 3 \times 10^3$ s, after which there is a reduction in n with further increase in time. In contrast, the results at 10 and 50 mM KNO_3 show an exponential increase in n with increasing time as predicted by theory. The results at 1 mM KNO_3, could not be fitted to obtain j_{ads} and j_{des} (Fig. 1a). On the other hand, the results at 10 and 50 mM KNO_3 could be fitted by Eqs. (5–7) and are shown in Figs. 1b and c.

The results at 1 mM KNO_3 at various shear rates are shown in Fig. 2. There does not seem to be a regular trend on the $n - t$ curve as the shear rate is increased. At 15 s^{-1}, n shows an exponential increase with increase in t. At 50 and 100 s^{-1} there seems to be a distinct maximum in the $n - t$ curve, which becomes less significant as the shear rate is further increased to 200 s^{-1}. The results for the influence of shear rate on n at 10 and 50 mM KNO_3 have the same trend as shown in Fig. 1b and c.

The initial deposition rates j_0, the dimensionless blocked areas γ (expressed as the ratio between the blocked area and the cross-sectional area of a particle), the desorption rate coefficients β, and the numbers of adhering particles in the stationary state n_∞, calculated by using the iterative least square fitting procedure described, are given in Table 1 for different shear rates and ionic strengths. The experiments were carried out in

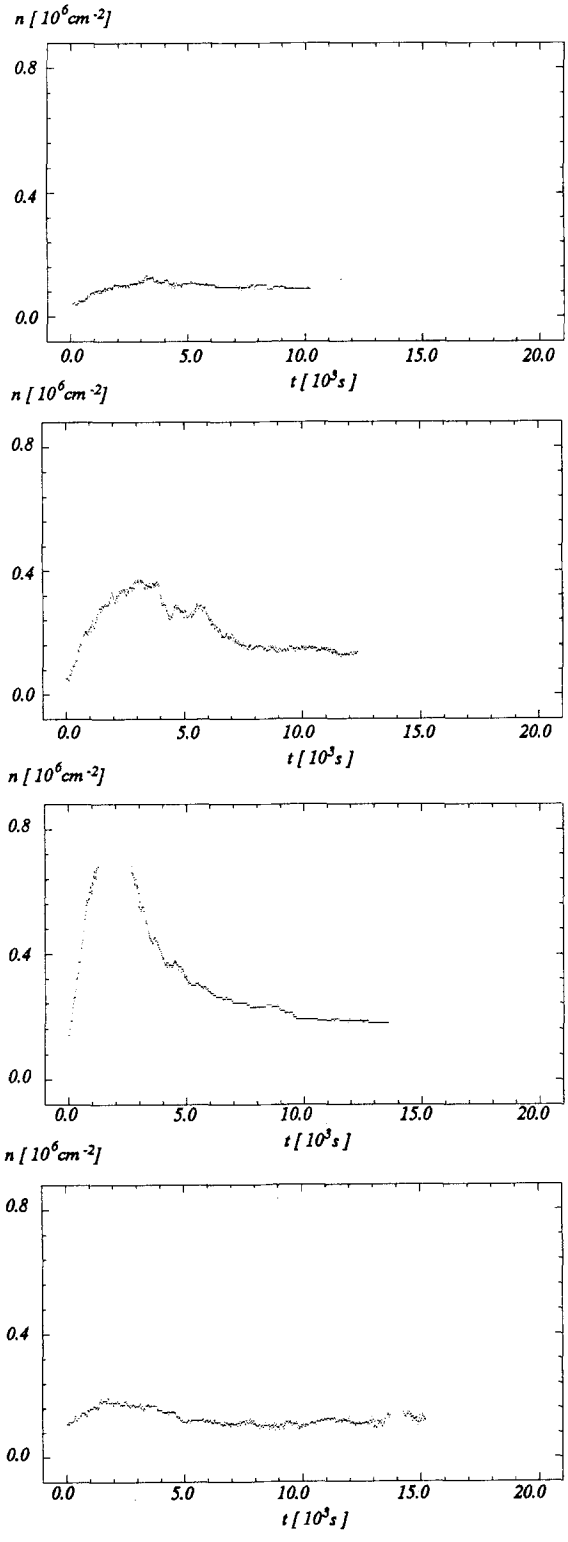

Fig. 2. Examples of the oscillatory behavior in time of the number of polystyrene particles adhering to a glass collector as a function of time at an ionic strength of 1 mM. From top to bottom the shear rates are 15, 50, 100 and 200 s^{-1}

duplicate and they coincided with each other within 25–35%.

From Table 1, it can be seen that the initial deposition rates increase, with increasing shear rate and ionic strength. Also the blocked areas and the desorption rate coefficients increase with increasing shear rate, but they decrease with increasing ionic strength. Similarly, the numbers of adhering particles in the stationary state increase with increasing ionic strength, but decrease with increasing shear rate.

Discussion

The initial deposition rate

In the initial stage of the deposition process, the surface coverage is low and, therefore, the initial deposition rates are mainly governed by particle-substratum interactions and are not influenced by interactions between flowing and adhering particles. From a theoretical point of view, it is interesting to compare the observed initial deposition rates with those calculated on the basis of the Smoluchowski–Levich approximation. Assuming that the additional hydrodynamic drag and lift forces a particle experiences while approaching a surface are overcome by attractive Van der Waals forces, and neglecting electrostatic interactions, the deposition efficiency ratio, i.e., the ratio between experimentally observed and theoretically calculated deposition rates can be expressed as [20]

$$\frac{Sh_{0,\mathrm{exp}}}{Sh_{0,\mathrm{theo}}} = \frac{\dfrac{j_0 a}{D_\infty c}}{\dfrac{1}{\Gamma(4/3)}\left(\dfrac{2}{9}\dfrac{Pe}{\bar{x}}\right)^{1/3}}, \tag{8}$$

in which a is the particle radius, c the particle concentration in the suspension, D_∞ the diffusion coefficient of particles sufficiently far from the collector surface, $\bar{x} = x/b$, the dimensionless distance from the entrance of the flow chamber, b the half channel depth of the flow chamber and Pe the dimensionless Peclet number for deposition of colloidal particles in a parallel plate flow chamber as defined by Adamczyk and Van de Ven [20]

$$Pe = \frac{3V_m a^3}{2b^2 D_\infty}, \tag{9}$$

Table 1. Initial deposition rates j_0, dimensionless blocked areas γ, desorption rate coefficients β and numbers of particles adhering to glass in the stationary state n_∞ in potassium nitrate solutions

Ionic strength (mM)	Shear rate (s^{-1})	j_0 ($cm^{-2}s^{-1}$)	γ	β ($10^{-6}s^{-1}$)	n_∞ ($10^6 cm^{-2}$)
1[a])	15	66	(705)	(214)	0.26
	50	143	(1151)	(265)	0.16
	100	331	(1222)	(461)	0.18
	200	349	(2374)	(761)	0.04
10	15	397	7(29)[b])	7	3.35
	50	378	493	30	1.13
	100	435	564	26	0.27
	200	469	870	49	0.22
50	15	450	10(23)	11	15.54
	50	520	30(26)	37	6.20
	100	793	33(35)	35	4.64
	200	711	564	58	0.51

[a]) β and A_1 should be considered with caution for the experiments carried out at 1 mM KNO_3, since for these experiments no exact fit of the data to Eqs. (5–7) could be obtained due to an oscillatory behavior in time of the number of adhering particles. However, j_0 was reliably obtained from the initial, linear time dependence of $n(t)$

[b]) Blocked area obtained from the local pair distribution function $g(x, y)$ are given between brackets behind the blocked areas obtained from deposition kinetics

Table 2. Deposition efficiencies expressed as ratio between the experimentally observed and theoretically calculated Sherwood numbers

Peclet number (10^{-3})	Ionic strength (mM KNO_3)		
	1	10	50
2.1	0.14	0.82	0.92
6.9	0.19	0.52	0.72
13.8	0.37	0.48	0.87
27.7	0.30	0.41	0.62

with V_m the mean velocity of the flow in the parallel plate flow chamber.

The results of the above calculations are summarized in Table 2. At the two high ionic strengths the deposition efficiency ratios decrease with increasing Peclet numbers, whereas at the low ionic strength the deposition efficiency ratio increases slightly with increasing Peclet numbers. This trend is difficult to explain since one would expect a reduction in deposition efficiency with increasing flow rate, due to increasing hydrodynamic lift and drag forces. It may be that at low ionic strength one needs to overcome the potential barrier between the particle and the surface to allow adhesion to occur. This may be facilitated at high shear rate (also kinetic flocculation).

Another possible indication of the cause increasing deposition efficiency ratio comes from the theoretical explanation of the oscillatory behavior of $n(t)$ observed at low ionic strength. Dabros and Van de Ven [1] have shown that, in case the interaction forces between an adhering particle and a collector surface become weaker in time, the deposition rate becomes a damped oscillating function. Obviously, the interaction forces are relatively stable at high ionic strength due to the predominant influence of attractive Van der Waals forces. Since Van der Waals forces are hardly affected by ionic strength, we envisage that at low ionic strength weakening of the total adhesive force will occur by variations in electrostatic interactions.

The deposition efficiency ratio clearly increases with increasing ionic strength. This trend is what one should expect since by increasing the ionic strength, the potential barrier is reduced and deposition efficiency is increased [6, 17, 18, 21, 22]. Under these (barrierless) conditions the deposition efficiency ratio quite closely follows the Smoluchowski–Levich approximation.

The desorption rate coefficient

Desorption of colloidal particles from collector surfaces depends on the shape of the interaction

potential function, i.e., the height of the potential barrier and the depth of the potential well, the thermal motion of the adhering particles [23–25], hydrodynamic lift and drag forces [26, 27], and collisions between flowing and adhering particles [3].

The increase in desorption rate with increase in shear rate is what would be expected from a consideration of the hydrodynamic forces, which increase with increase of shear rate. In addition, the number of collisions between the flowing and adhering particles will also increase with increase of shear rate. These two effects will lead to an increase in desorption rate as found experimentally. The effect of electrolyte on desorption should be considered in terms of the balance between electrostatic forces and hydrodynamic interactions. Increasing electrolyte concentration results in a reduction of the energy barrier and this should increase the number of adhering particles. However, the reduction in energy barrier should also facilitate particle removal. The results in Table 1 show an opposite trend, i.e., a reduction in desorption rate with increase in electrolyte concentration, indicating that the first effect must be overriding and one should take the shape of the interaction potential function into account. This means that the increased height of the potential barrier at low ionic strength is of less importance with regard to desorption than the overall change in the shape of the interaction potential function due to variation in ionic strength.

The blocked area

The dimensionless blocked areas, γ, as presented in Table 1, show major variations with ionic strength and shear rate. In the absence of electrostatic repulsions, i.e., at high ionic strengths, blocked areas are considerably smaller than in the presence of electrostatic repulsions, i.e., at low ionic strengths. Furthermore at each ionic strength the blocked areas increase with increasing shear rate due to increasing hydrodynamic interactions between flowing and adhering particles.

The dimensionless blocked areas published [9] in the literature so far range from 10–30 in the absence of electrostatic interactions between collector surfaces and particles and from 20–60 when electrostatic repulsion exist between collector surfaces and particles [1, 3, 31]. Our results approach these values only at the high 50 mM KNO_3 (except at high shear rates). The blocked areas at 1 mM KNO_3 are clearly unrealistic, as this is due to the oscillation obtained for the $n - t$ results. However at 10 mM KNO_3, with the exception of the low shear rate value, the results are still high. It is believed that the desorption rate measured in this case is underestimated. Possibly with a faster image analysis system, higher desorption rates would have been observed, resulting in a smaller influence of blocking on the deposition process and correspondingly lower values for the blocked areas.

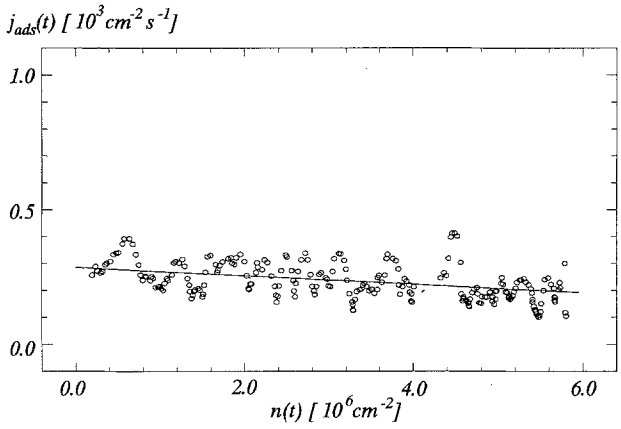

Fig. 3. $j_{ads}(t)$ as a function of $n(t)$ for deposition of polystyrene particles on a glass collector from a potassium nitrate solution with an ionic strength of 50 mM and a shear rate of 50 s^{-1}

It has been suggested that the blocked area per particle depends on the degree of surface coverage due to overlap [4, 12]. However, for the present experimental conditions overlap is not likely, since $j_{ads}(t)$ is a linear function of $n(t)$ according to Eq. (3), as can be seen from Fig. 3 showing a selected example of the relation between $j_{ads}(t)$ and $n(t)$. The line drawn is the average result of the experimental data which are shown in the figure.

Recently, we proposed that blocked areas could also be estimated from the local pair distribution functions, $g(x, y)$, as can be calculated from an analysis of the spatial arrangement of adhering particles on collector surfaces [11]. Due to statistical limitations, such an analysis could only be done for the present set of experiments when n_∞

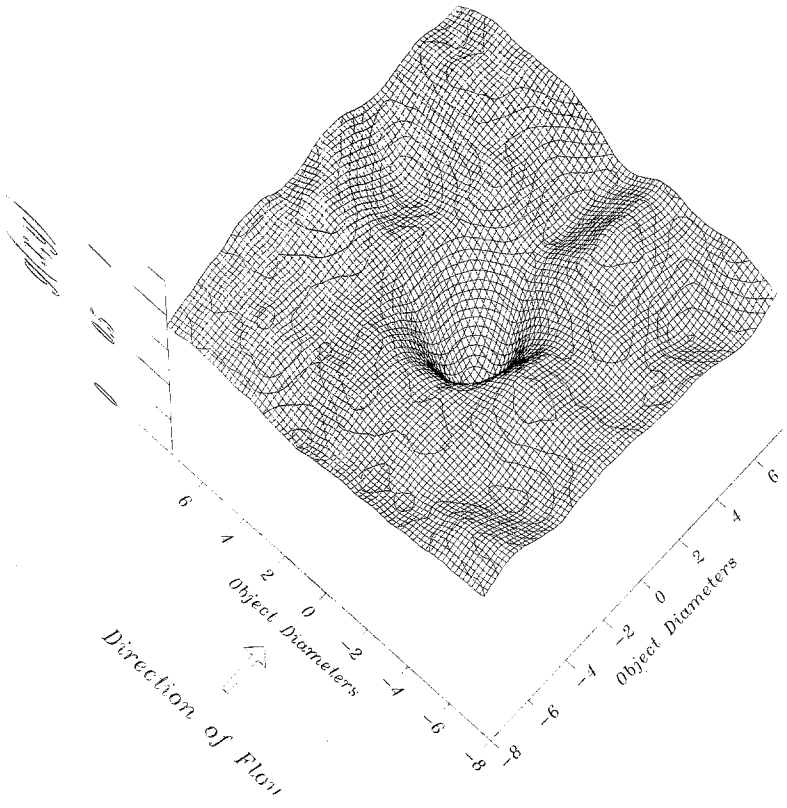

Fig. 4. Local pair distribution function $g(x, y)$ obtained from an analysis of the spatial arrangement of polystyrene particles adhering to glass for the experiment done at an ionic strength of 50 mM and a shear rate of $100\ s^{-1}$. The arrow indicates the direction of flow. An asymmetrical zone of lower average density is clearly visible around the central particle

exceeded $3 \times 10^6\ cm^{-2}$. Figure 4 shows $g(x, y)$ for a selected example and we emphasize the following features: $g(x, y)$ has a rotationally asymmetrical shadow-zone of low density around the central particle elongated in the direction of flow and is symmetrical transverse to the direction of flow. Since we are measuring at low regimes, flow lines are symmetrical in front of and behind particles, thus one should expect symmetrical blocked areas. However, due to electrostatic repulsions between flowing and adhering particles, the flowing particles can be pushed away from the collector surface into higher lying flow lines, thus reducing its probability to adsorb behind an adhering particle [32, 33].

Assuming that blocked areas correspond with local densities from local pair distribution function around a central particle with an average density less than 1.0, estimates of the blocked areas can be calculated as presented in Table 1 in between brackets. Results of duplicate runs coincided within 15%. From these results it can be seen that blocked areas at high surface coverage correspond well with those obtained from the deposition kinetics.

Conclusion

Summarizing, we can draw the following conclusions from the results of this study:

– Simultaneous measurement of adsorption and desorption of colloidal particles on collector surfaces can result in a description of the deposition process in terms of the initial deposition rate, the desorption rate coefficient, and the blocked area.

– The experimentally observed initial deposition rates corresponded well with the initial deposition rates calculated on the basis of the Smoluchowski–Levich approximation. However, this correspondence decreases with increasing shear rates and decreasing ionic strengths, due to increased hydrodynamic interaction and electrostatic repulsions, respectively.

– At high ionic strength, the interaction between adhering particles and the collector surface is relatively stable due to the predominant influence of attractive Van der Waals forces, whereas at low ionic strength the total adhesive force varies due to variations in electrostatic interactions, resulting in an oscillatory behavior of $n(t)$.

– Blocked area increases with increasing shear rate, and with decreasing ionic strength. Furthermore, for those cases in which a sufficient high number of adhering particles was found, blocked areas calculated from the deposition kinetics corresponded well with those derived from an analysis of the spatial arrangement of adhering particles.

Acknowledgment

The authors are greatly indebted to Dr. Th.F. Tadros for critically commenting on the manuscript.

References

1. Dabros T, Van de Ven TGM (1982) J Colloid Interface Sci 89:232
2. Hinrichsen EL, Feder, Jøssang T (1986) J Statistical Ph 44:793
3. Varennes S, Van de Ven TGM (1987) PCH Phys Chem Hydrodyn 9:537
4. Schaaf P, Talbot J (1989) J Chem Phys 91:4401
5. Sjollema J, Busscher HJ, Weerkamp AH (1989) J Microbiol Methods 9:79
6. Van de Ven TGM (1989) Colloids Surf 39:107
7. Adamczyk Z, Zembala M, Siwek B, Warszynski P (1990) J Colloid Interface Sci 140:123
8. Meinders JM, Noordmans J, Busscher HJ (1992) J Colloid Interface Sci 152:265
9. Dabros T (1989) Colloids Surf 39:127
10. Sjollema J, Van der Mei HC, Uyen HM, Busscher HJ (1990) FEMS Microbiol Letters 69:263
11. Busscher HJ, Noordmans J, Meinders J, Van der Mei HC (1991) Biofouling 4:71
12. Adamczyk Z, Siwek B, Zembala M (1991) Biofouling 4:89
13. Hubbe MA (1985) Colloids Surf 16:227
14. Sharma MM, Chamoun H, Sita Rama Sarma DSH, Schechter RS (1992) J Colloid Interface Sci 149:121
15. Kallay N, Tomić M, Biškup B, Kunjasic I, Matijević E (1987) Colloids Surf 28:185
16. Sjollema J, Busscher HJ, Weerkamp AH (1989) J Microbiol Methods 9:73
17. Brouwer WM, Zsom RLJ (1987) Colloids Surf 24:195
18. Sjollema J, Busscher HJ (1990) Colloids Surf 47:323
19. Meinders JM, Van der Mei HC, Busscher HJ (1992) J Microbiol Methods 16:119
20. Adamczyk Z, Van de Ven TGM (1981) J Colloid Interface Sci 80:340
21. Hull M, Kitchener JA (1969) Trans Faraday Soc 65:3093
22. Sjollema J, Busscher HJ (1989) J Colloid Interface Sci 132:382
23. Hubbe MA (1987) Colloids Surf 25:325
24. Dahneke B (1975) J Colloid Interface Sci 50:89
25. Dahneke B (1975) J Colloid Interface Sci 50:194
26. Goldman AJ, Cox RG, Brenner H (1967) Chem Eng Sci 22:637
27. Goldman AJ, Cox RG, Brenner H (1967) Chem Eng Sci 22:653
28. Kallay N, Bišku B, Tomić M, Matijević E (1986) J Colloid Interface Sci 114:357
29. Reynolds PA, Goodwin JW (1987) Colloids Surf 23:273
30. Van de Ven TGM (1988) J Colloid Interface Sci 124:138
31. Dabros T, Van de Ven TGM (1983) Colloid Polym Sci 261:694
32. Małysa K, Dabros T, Van de Ven TGM (1986) J Fluid Mech 162:157
33. Dabros T, Van de Ven TGM (1992) Int J Multiphase Flow 18:751

Received March 8, 1993;
accepted May 16, 1993

Authors' address:

Dr. H.J. Busscher
Laboratory for Materia Technica
University of Groningen
Antonius Deusinglaan 1
9713 AV Groningen, The Netherlands